The Plant Cell, Vol. 13, 1987–2004, September 2001, www.plantcell.org © 2001 American Society of Plant Biologists

RESEARCH ARTICLE

PDE1 Encodes a P-Type ATPase Involved in Appressorium-Mediated Plant Infection by the Rice Blast Fungus *Magnaporthe grisea*

Pascale V. Balhadère and Nicholas J. Talbot[1]

School of Biological Sciences, University of Exeter, Washington Singer Laboratories, Perry Road, Exeter EX4 4QG, United Kingdom

Plant infection by the rice blast fungus *Magnaporthe grisea* is brought about by the action of specialized infection cells called appressoria. These infection cells generate enormous turgor pressure, which is translated into an invasive force that allows a narrow penetration hypha to breach the plant cuticle. The Magnaporthe *pde1* mutant was identified previously by restriction enzyme–mediated DNA integration mutagenesis and is impaired in its ability to elaborate penetration hyphae. Here we report that the *pde1* mutation is the result of an insertion into the promoter of a P-type ATPase-encoding gene. Targeted gene disruption confirmed the role of *PDE1* in penetration hypha development and pathogenicity but highlighted potential differences in *PDE1* regulation in different Magnaporthe strains. The predicted *PDE1* gene product was most similar to members of the aminophospholipid translocase group of P-type ATPases and was shown to be a functional homolog of the yeast ATPase gene *ATC8*. Spatial expression studies showed that *PDE1* is expressed in germinating conidia and developing appressoria. These findings implicate the action of aminophospholipid translocases in the development of penetration hyphae and the proliferation of the fungus beyond colonization of the first epidermal cell.

INTRODUCTION

One of the principal reasons why pathogenic fungi are so successful at causing plant disease is their ability to penetrate the plant cuticle directly, often using specialized infection cells called appressoria (Mendgen et al., 1996). A wide variety of fungal pathogens form appressoria, and the development of these cells involves a complex morphogenetic program that results in rapid differentiation of a highly specialized structure (Dean, 1997). The rice blast fungus *Magnaporthe grisea* is an important pathogen of cultivated rice and has emerged as an experimental model for the study of plant infection processes (for reviews, see Howard and Valent, 1996; Hamer and Talbot, 1998). Magnaporthe develops dome-shaped appressoria, which form at the ends of germ tubes soon after spore germination on the leaf surface. Appressoria attach strongly to the leaf and then generate enormous turgor pressure (up to 8 MPa), which is used to rupture the plant cuticle (Howard et al., 1991). The turgor inside appressoria is generated by a rapid increase in intracellular glycerol levels, which is maintained by a specialized cell wall layer containing melanin (Howard and Ferrari, 1989; de Jong et al., 1997). If melanin biosynthesis is blocked, either by chemical intervention or mutation, then Magnaporthe is unable to penetrate the plant surface and cannot cause disease (Chida and Sisler, 1987; Chumley and Valent, 1990).

How such enormous cellular turgor is translated into the substantial invasive force necessary to breach the plant cell wall is not clear, but it appears to involve polarization of the cytoskeleton to the point of infection and localized cell wall modification (Bourett and Howard, 1990, 1992; Bechinger et al., 1999). A narrow penetration hypha forms at the base of the appressorium, and this narrow cylindrical structure (also known as a penetration peg) breaks the cuticle layer and the epidermal cell wall (Bourett and Howard, 1990).

Formation of the penetration hypha by Magnaporthe appressoria is likely to be accompanied by severe membrane stress and rapid cell wall biosynthesis at the hyphal apex, because the enormous cellular turgor of the appressorium is focused in the elongating cell (Talbot, 1995). A mitogen-activated protein kinase–encoding gene, *MPS1*, is required for appressorium-mediated penetration (Xu et al., 1998). Mps1 is functionally related to the Slt2/Mpk1 kinase from *Saccharomyces cerevisiae*, which is responsible for the regulation of cell wall growth under conditions of membrane stress (Davenport et al., 1995). The rapidly advancing penetration hypha ruptures the plant epidermal cell wall and then differentiates into a bulbous infection hypha, a branched

[1] To whom correspondence should be addressed. E-mail n.j.talbot@exeter.ac.uk; fax 1392-264668.

structure that fills the initial plant cells encountered, before ramifying throughout the leaf tissue (Heath et al., 1990). During this stage of rice blast disease, fungal hyphae grow both between and within plant cells, and disease symptoms appear 3 to 5 days after initial infection. Although regulators of appressorium development have been identified in Magnaporthe (Hamer and Talbot, 1998), the effectors of penetration peg formation and the cellular processes required for elaboration of specialized infection hyphae are unknown.

In this report, we present the identification of a gene, *PDE1*, that encodes a protein involved in penetration hypha production by appressoria of Magnaporthe. To isolate *PDE1*, we adopted a mutagenic approach. Recently, we reported the preliminary results of a mutant screen using restriction enzyme–mediated insertion (REMI) mutagenesis, which identified five novel pathogenicity mutants (Balhadère et al., 1999). Among the mutants we identified was a penetration-defective mutant called *pde1*. The *pde1* mutant exhibited reduced appressorium-mediated penetration and produced very few disease symptoms when inoculated onto a susceptible plant host (Balhadère et al., 1999). In this article, we report that *PDE1* encodes a P-type ATPase belonging to a family of aminophospholipid translocases. These integral membrane proteins are required for the maintenance of phospholipid asymmetry in biological membranes. The PDE1 protein appears to play a critical role in the ability of Magnaporthe to produce a functional penetration hypha during plant infection. This observation suggests that membrane asymmetry may be an important requirement for the development of infection hyphae by phytopathogenic fungi.

RESULTS

PDE1 Is Required for the Proliferation of Magnaporthe in Barley Leaf Tissue

The *pde1* mutant was isolated as a pathogenicity mutant of Magnaporthe and was shown previously to be defective in its ability to penetrate epidermal cell layers and grow in plant tissue (Balhadère et al., 1999). To determine the extent to which the colonization of plant tissue is impeded in a *pde1* mutant, we performed a comparative analysis of the plant infection process in a *pde1* mutant and an isogenic wild-type strain of Magnaporthe. Barley seedlings of the susceptible cultivar Golden Promise were infected with the wild-type Magnaporthe strain 35-R-24 and the REMI *pde1* mutant strain 2029 and examined using low-temperature scanning electron microscopy. The infection process was allowed to progress for 72 hr, at which time blast disease symptoms normally appear. A representative section through a barley leaf infected with the wild-type strain 35-R-24 is shown in Figure 1A. An appressorium is visible on the leaf surface, and infection hyphae have ramified throughout the epidermal and mesophyll layers of the leaf and are present both within and between plant cells. In contrast, at the same time, the majority of the appressoria (~90%) formed by the *pde1* mutant 2029 appeared as shown in Figure 1B, with no visible signs of having produced a penetration peg and no disruption of the leaf cuticle. In a small number of cases, appressoria of the *pde1* mutant 2029 did produce bulbous infection hyphae, as shown in Figure 1C, but these did not progress beyond the first epidermal cell encountered. The *PDE1* gene, therefore, encodes a protein involved in penetration peg formation and proliferation of the fungus beyond colonization of the first epidermal cell.

The *pde1* Mutation Is the Result of a Promoter Insertion

Genetic analysis previously showed that the *pde1* mutation cosegregates with the presence of an insertion of the pCB1003 plasmid used in REMI mutagenesis (Balhadère et al., 1999). To isolate the *PDE1* gene, the inserted copy of pCB1003 was excised from the genome along with flanking DNA from the point of insertion. A 3.2-kb ClaI fragment, which contained a section of chromosomal DNA and the pCB1003 inserted vector, was identified at the *pde1* insertion locus, as shown in Figure 2A. Magnaporthe genomic DNA was isolated and digested with ClaI before being religated and transformed into *Escherichia coli*. The recovered plasmid was sequenced, and the chromosomal DNA fragments were used to screen a Magnaporthe genomic library. A genomic clone was restriction mapped, and a 6.94-kb PstI-SalI fragment was subcloned and completely sequenced. This analysis, and complementary restriction mapping of the REMI mutant 2029, showed that the original insertion had occurred 165 bp upstream of a large open reading frame, as shown in Figure 2B. To determine whether this open reading frame corresponded to the *PDE1* gene, a genetic complementation experiment was performed.

We amplified and cloned a 6.48-kb DNA fragment spanning the entire candidate locus and 1.47-kb of upstream promoter sequence (see Methods) and introduced this into the Magnaporthe *pde1* mutant 2029-32 by cotransformation with a vector bestowing sulfonylurea resistance. A number of transformants were selected and analyzed by DNA gel blotting to confirm the introduction of a single copy of the putative *PDE1* locus (data not shown). Transformants were tested in cuticle penetration assays using sterilized onion epidermis and seedlings of the barley cultivar Golden Promise. Penetration of onion epidermis (Chida and Sisler, 1987) and of intact barley epidermis was analyzed by microscopy, and representative results from one of the pPDE1 transformants, PVB6.1, and the isogenic *pde1* mutant strain 2029-32 are shown in Figure 3A. The frequency of penetration of onion epidermis by PVB6.1 was significantly greater than that of the *pde1* mutant 2029-32 ($\chi^2 = 367.2$, $df = 1$, $P < 0.001$) but was not significantly different from the frequency of penetration of the wild type ($\chi^2 = 4.75$, $df = 1$, $P = 0.01$). A similar result was obtained for the penetration of intact barley

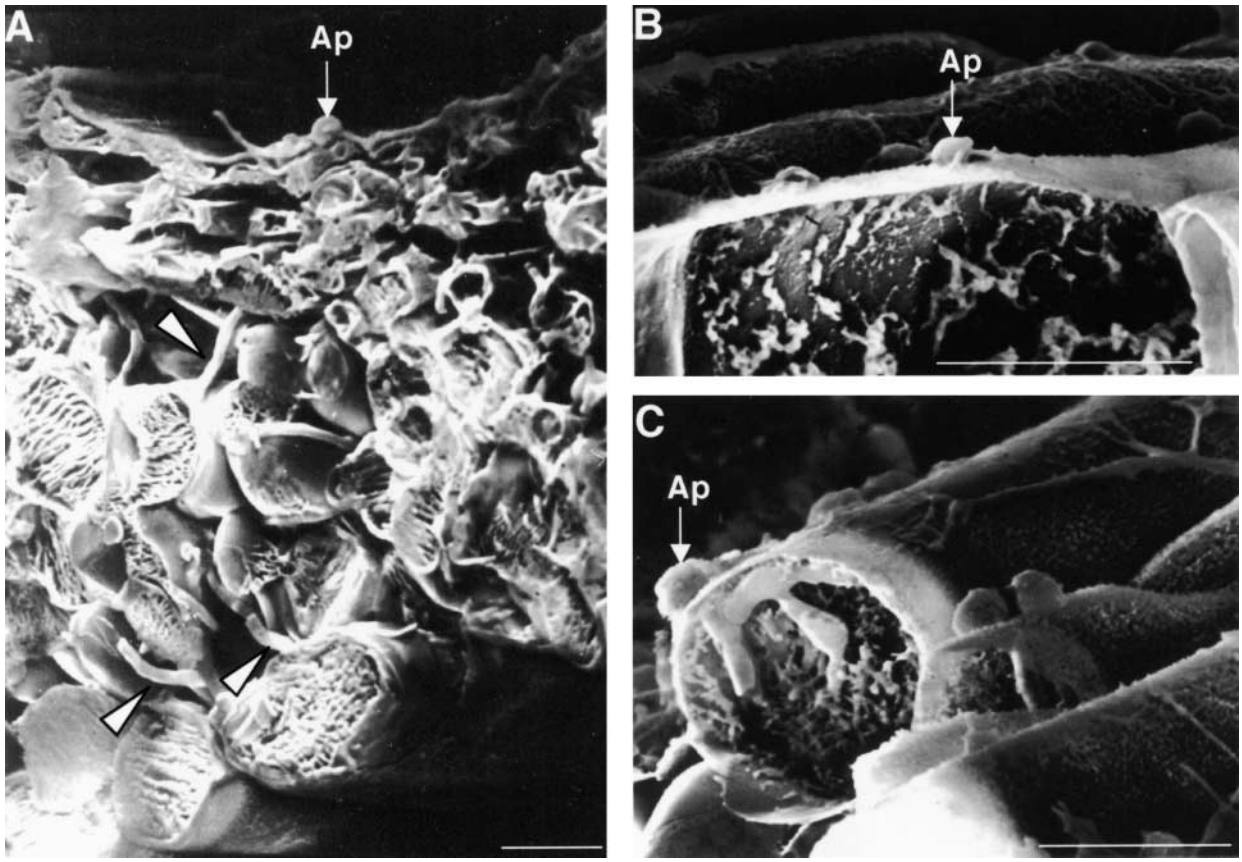

Figure 1. Infection of Barley by Wild-Type and *pde1* Mutant Strains of Magnaporthe.

Conidia were inoculated on excised barley leaves (cv Golden Promise) and incubated at 24°C for 72 hr. Leaves were plunge frozen in nitrogen slush and then fractured at low temperature on the stage of a scanning electron microscope to reveal internal detail. Bars = 25 μm.

(A) Barley leaf inoculated with the wild-type Magnaporthe strain 35-R-24. An appressorium (Ap) is visible on the leaf surface, and infection hyphae are present throughout the epidermal and mesophyll cell layers (arrowheads).

(B) Barley leaf inoculated with *pde1* mutant 2029. An appressorium is visible on the leaf surface (Ap) but has not developed a penetration hypha. Approximately 90% of the appressoria observed showed this appearance after 72 hr.

(C) Barley leaf inoculated with *pde1* mutant 2029. An appressorium (Ap) has penetrated the leaf and formed an infection hypha that has arrested growth within the first epidermal cell.

cuticles (Figure 3A). Pathogenicity assays also were performed by spray inoculation of barley seedlings, and disease symptom formation was restored completely in PVB6.1 (data not shown). Together, these results suggest that the cause of the *pde1* mutation in the REMI mutant 2029 is an insertion of the pCB1003 plasmid in the promoter of a 4.5-kb gene.

Because the *pde1* mutation was attributable to a promoter insertion, we decided to perform targeted gene disruption of *PDE1* to ensure the production of a loss-of-function mutant. We also wanted to test the effect of the *pde1* mutation in a rice pathogenic strain of Magnaporthe. The gene disruption was performed by constructing a vector containing the hygromycin phosphotransferase–encoding gene cassette (*HPH*), which was subcloned by blunt-end ligation into a SmaI site found at the 5′ end of the putative *PDE1* open reading frame (see Methods). The resulting gene disruption allele contained a 1.4-kb insertion within the first exon of the *PDE1* gene. We reasoned that such a large insertion in the first exon of the gene would be sufficient to ensure the loss of gene function. The pPde1::Hph vector was linearized and transformed into Magnaporthe strain Guy11. The presence of the *pde1*::*Hph* insertion allele (Figure 2D) was verified by DNA gel blotting. Hybridization analysis with probe pSKPS1 showed the presence of a 2.6-kb PstI fragment in the wild-type strain Guy11 (Figure 2E, lane 1). Four of the transformants (PV1, PV2, PV3, and PV4) contained a larger hybridizing 4.0-kb fragment, which is indicative of a gene disruption (Figure 2E, lanes 3 to 6). The

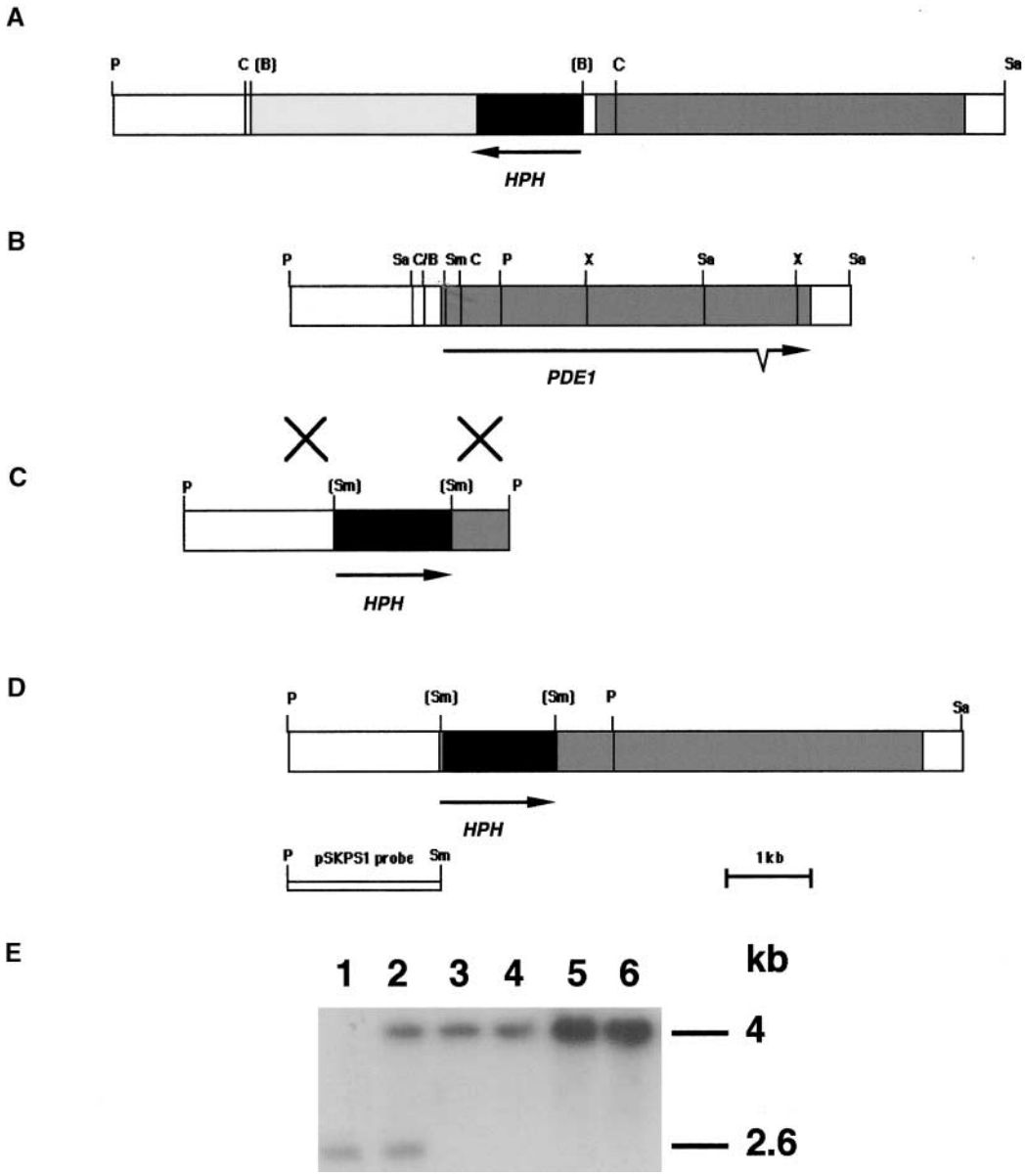

Figure 2. Organization of the *PDE1* Locus and Targeted Gene Disruption.

(A) Restriction map of the insertional mutant locus of *pde1* mutant 2029. A copy of plasmid pCB1003 was introduced into Magnaporthe by REMI to create the hygromycin B–resistant mutant 2029 (Balhadère et al., 1999). The integration resulted in loss of the BamHI sites at each end of the integrated plasmid. The position and orientation of the hygromycin B resistance gene cassette (Carroll et al., 1994) are indicated (*HPH*). pCB1003 integration was found to have occurred 165 bp upstream of a large open reading frame (gray shading). ClaI sites found on either side of the integrated plasmid were used to excise a fragment of the insertion locus.

(B) Restriction map of the *PDE1* locus isolated as a 6.94-kb PstI-SalI fragment from a Magnaporthe strain Guy11 genomic library. The *PDE1* locus contains a 4575-bp open reading frame interrupted by a single intron at positions 3927 to 3997. The arrow indicates the orientation of the open reading frame and the position of the intron.

(C) Targeted gene disruption vector pPde1::Hph. The vector was made by excising a 2.6-kb PstI fragment at the 5′ end of *PDE1* and inserting the hygromycin B resistance gene cassette (*HPH*) in a SmaI site.

(D) Restriction map of the *pde1*::*Hph* disruption allele showing the position of the hygromycin resistance gene cassette (*HPH*) at the 5′ end of the *PDE1* open reading frame.

(E) DNA gel blot analysis of pPde1::Hph transformants. Genomic DNA was prepared from the wild-type strain Guy11 (lane 1), the ectopic integration transformant PV9 (lane 2), and four *pde1*::*Hph* mutant transformants, PV1, PV2, PV3, and PV4 (lanes 3 to 6, respectively). Genomic DNA was digested with PstI and separated on a 0.8% agarose gel. The blot was probed with pSKPS1.

The Xs between **(B)** and **(C)** indicate a crossover event. B, BamHI; C, ClaI; P, PstI; Sa, SalI; Sm, SmaI; X, XhoI.

remaining transformants showed hybridization to both PstI fragments, indicating ectopic insertion of the gene replacement vector (Figure 2E, lane 2). The insertion allele from transformant PV1 was sequenced (data not shown), and it confirmed that the hygromycin phosphotransferase gene had not introduced any new in-frame translation initiation codons that might allow translation of a truncated PDE1 protein. Furthermore, four stop codons were present within the last 80 bp of the insertion, ensuring that downstream translation was prevented in any reading frame (see Methods and Figure 2C).

The effect of the *pde1*::*Hph* mutation on pathogenesis was tested by spray inoculating seedlings of the susceptible rice cultivar CO-39 with uniform concentrations of conidia from either the wild-type Magnaporthe strain or an isogenic *pde1*::*Hph* mutant and allowing blast disease to progress. Rice plants infected with *pde1*::*Hph* mutants showed a reduction in the number of disease lesions compared with the wild type, as shown in Figures 3B and 3C, and produced only small necrotic lesions. Five independent *pde1*::*Hph* transformants were assessed with identical results (data not shown). A quantitative analysis (Figure 3F) showed that the number of disease lesions was reduced significantly in plants inoculated with the *pde1*::*Hph* mutant PV1 compared with those infected with Guy11 ($F = 33.7$, $P = 0.001$). To ensure that the virulence defect was not associated with reduced growth of the fungus, the vegetative growth of Guy11 and PV1 was recorded in axenic culture and showed no significant difference at either 3 days ($F = 1.46$, $P > 0.05$) or 5 days ($F = 3.17$, $P > 0.05$) after inoculation.

The rice pathogenic Magnaporthe strain Guy11 is also pathogenic on barley cultivar Golden Promise; therefore, we assessed the pathogenicity of *pde1*::*Hph* mutants on this alternative grass host. To our surprise, all of the *pde1*::*Hph* mutants tested were able to cause disease symptoms identical to the wild type on this grass host (Figures 3D and 3E). To investigate the possible reasons for the observed differences in disease symptom production on rice and barley, we performed cuticle penetration assays on the *pde1*::*Hph* mutant PV1 and Guy11 by using onion epidermis, barley leaves, and rice leaves (Figure 3A). We found a clear difference in the ability of PV1 to penetrate onion epidermis and a small but statistically significant reduction in the ability to penetrate rice leaves after 48 hr (90% successful penetration by appressoria of Guy11 compared with 74% for PV1; $F = 5.31$, $P = 0.05$). In contrast, there was no significant difference between the ability of appressoria of Guy11 and PV1 to penetrate barley epidermis (Figure 3A). To determine whether the differences in penetration were associated with differences in the infection-related development of PV1 and Guy11, we assayed appressorium development on each leaf surface and on artificial plastic surfaces. No differences were observed in the number of appressoria produced by each strain. However, we did observe a delay in the early stages of spore germination (11% germination of conidia of PV1 after 2 hr of incubation, compared with 43% germination of Guy11 conidia; $F = 18.42$, $P < 0.05$). Germ tube elongation proceeded normally after this initial delay, and by 5 hr after inoculation, the frequency of germination was not significantly different (86% for PV1, 93% for Guy11). Thereafter, the time and frequency of appressorium formation proceeded normally. We conclude that *PDE1* encodes a virulence determinant required for the efficient infection of barley seedlings by strain 35-R-24 and of rice by Guy11. Our results also indicate that *PDE1* may act differently in Magnaporthe strain backgrounds because a *pde1*::*Hph* mutation has no effect on Guy11 virulence toward barley.

PDE1 Encodes a P-Type ATPase

Sequencing of the 6.94-kb PstI-SalI fragment spanning the *PDE1* locus revealed the presence of a large single open reading frame of 4.6 kb interrupted by one intron. The putative *PDE1* translation product showed similarity to P-type ATPases and was 31% identical and 63% similar to the *S. cerevisiae ATC8* gene (SWISS-PROT accession number Q12674; yeast genome accession number Ymr162c), as shown in Figure 4. The *PDE1*-encoded protein has a predicted molecular mass of 166.9 kD and contains 10 predicted membrane-spanning domains and all of the conserved features expected of a P-type ATPase (Lutsenko and Kaplan, 1995). A scheme of the putative translation product and the related *ATC8* product is shown in Figure 5A. The PDE1 protein has five predicted extracytoplasmic domains connected to membrane-spanning regions. The predicted cytoplasmic domains of PDE1 contain all five of the known P-type ATPase consensus motifs, including an ATP binding site at position 978 and a phosphorylation site at position 488, as shown in Figure 5A. Phylogenetic analysis showed that the *PDE1* product is most closely related to P-type ATPases of the DRS2 family of putative aminophospholipid translocases, as shown in Figure 5B. It is clearly distinct from the other main classes of P-type ATPases, including the H^+-ATPases, Ca^{2+}-ATPases, and Na^+-ATPases (all P_2 type), Cu^{2+}-ATPases (P_1 type), and P_4-type ATPases that have been identified so far (reviewed by Catty et al., 1997; Paulsen et al., 1998).

To determine whether *PDE1* was functionally related to P-type ATPases of the aminophospholipid translocase group, we subcloned a 4.6-kb intronless fragment of the *PDE1* gene into pYES2 for expression under the *S. cerevisiae GAL1* promoter in the *atc8Δ* mutant YB853 (Ashrafi et al., 1998). The *atc8Δ* mutant YB853 was generated in a screen for interactions affecting the N-myristoylation pathway in yeast, but no mutant phenotype was reported in that study (Ashrafi et al., 1998) or was known to its authors (K. Ashrafi, personal communication). Therefore, we performed a detailed comparison of the growth and development of YB853 with an isogenic wild-type yeast strain YB332. We found a consistent reduction in the growth of the *atc8Δ* mutant YB853 on minimal growth medium that could be assayed reproducibly in plate tests (see Methods). We used this

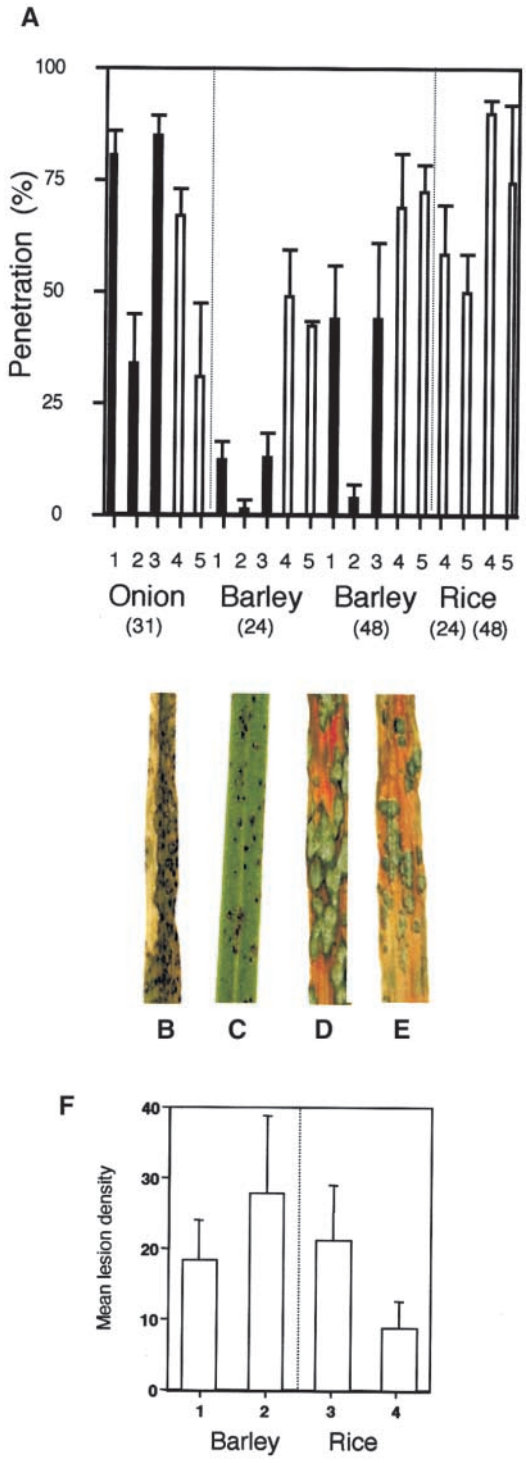

Figure 3. Appressorium-Mediated Penetration and Plant Infection Assays.

Appressorium-mediated penetration assays were performed using a modification of the method of Chida and Sisler (1987). Magnaporthe conidial suspensions were incubated on sterilized onion epidermis or intact barley and rice epidermis, and the percentage of appressoria that had penetrated the cuticle by elaboration of a penetration hypha was recorded after 31 hr for onion epidermis and after 24 and 48 hr for barley and rice epidermis. For plant infection assays, barley seedlings (cv Golden Promise) and rice seedlings (cv CO-39) were spray inoculated with conidial suspensions of Magnaporthe, and representative leaves were collected 72 hr after inoculation.

(A) Bar charts showing the percentage of appressorium penetration. 1, inoculation with wild-type strain 35-R-24; 2, *pde1* mutant 2029-32; 3, pPDE1 transformant PV6.1; 4, Guy11; 5, *pde1*::*Hph* mutant PV1.

(B) Rice leaf from a plant inoculated with wild-type strain Guy11.

(C) Rice leaf inoculated with a *pde1*::*Hph* mutant of Guy11, PV1.

(D) Barley leaf from a plant inoculated with wild-type strain Guy11.

(E) Barley leaf inoculated with a *pde1*::*Hph* mutant of Guy11, PV1.

(F) Bar chart showing the results of quantitative analysis of barley and rice infection assays. Mean lesion density values were recorded from 10 randomly chosen 5-cm leaf tips. 1, inoculation of barley with Guy11; 2, inoculation of barley with the *pde1Δ* mutant of Guy11, PV1; 3, inoculation of rice with Guy11; 4, inoculation of rice with the *pde1Δ* mutant, PV1. Bars indicate ±SD.

assay to determine whether the *atc8Δ* mutant could be complemented by the expression of Magnaporthe *PDE1*. Transformants carrying the *GAL1(p)*:*PDE1* construct were able to complement the *atc8Δ* mutant phenotype after induction of expression in the presence of galactose, as shown in Figure 6. We conclude that *PDE1* encodes a P-type ATPase that is functionally related to *ATC8*.

PDE1 Conservation in Guy11 and 35-R-24

Because of the observed differences in the mutant phenotype associated with the *pde1*::*Hph* insertion mutant of Guy11, PV1, and the original REMI mutant of 35-R-24, 2029, we performed sequence analysis of the *PDE1* allele from both Magnaporthe strain backgrounds (Figure 7). In total, we found 45 nucleotide differences between Guy11 and 35-R-24 in the 4.6-kb *PDE1* gene sequence (0.98% difference). These comprised 12 purine transitions, 20 pyrimidine transitions, three purine-to-pyrimidine transversions, nine pyrimidine-to-purine transversions, and one guanine deletion. These changes resulted in five nonsilent mutations, of which four were conservative substitutions with similar amino acids. The single nonconservative substitution was a valine (Guy11 allele) to serine (35-R-24 allele) mutation at position 535. All of the nonsilent mutations were found in sequences corresponding to the large cytoplasmic loop between transmembrane domains 4 and 5. All five P-type ATPase consensus sequences were conserved between both alleles. The intron contained a deletion and two of the transition mutations. Analysis of the *PDE1* promoter sequence up to position

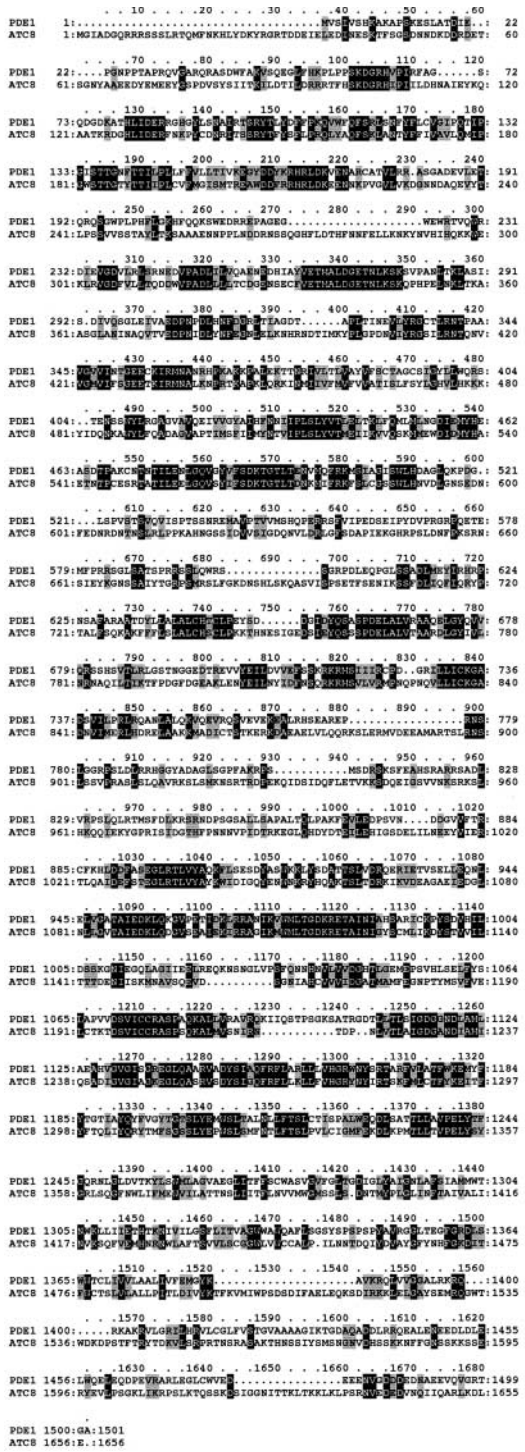

Figure 4. Predicted Amino Acid Sequence of the Magnaporthe *PDE1* Gene.

Amino acid sequence alignment of the predicted Magnaporthe PDE1 gene product with *S. cerevisiae* ATC8. Sequences were aligned with the ClustalW program (Thompson et al., 1994). Identical amino acids are shown on a black background, and similar amino acids are shown on a light gray background. Gaps in the sequences are indicated by dashes. *PDE1* has GenBank accession number AY026257.

−1465 revealed 39 nucleotide differences between Guy11 and 35-R-24 alleles (2.65% difference). The positions of putative transcription factor binding sites (see below) were conserved in both alleles. We conclude that a high level of conservation exists between alleles of *PDE1* from both Magnaporthe strain backgrounds investigated.

PDE1 Is Expressed during Appressorium Development

The expression of *PDE1* in Magnaporthe could not be detected by RNA gel blot analysis despite exhaustive efforts. Therefore, we analyzed the spatial and temporal control of *PDE1* gene expression by construction and expression of a *PDE1* promoter–green fluorescent protein (GFP) fusion in Magnaporthe. A 1.47-kb fragment of the *PDE1* promoter was amplified and subcloned in frame with the *sGFP* allele (Chiu et al., 1996), which has been shown to work well in Magnaporthe (Kershaw et al., 1998). The resulting construct was subcloned into a Magnaporthe transformation vector and introduced into Guy11 using hygromycin selection. Hygromycin-resistant transformants were identified and analyzed by DNA gel blot analysis. Four transformants (PVG1 to PVG4) carrying single-copy insertions were selected for further analysis. Expression of GFP in *PDE1(p):sGFP* transformants was detected in conidia and during appressorium development, as shown in Figure 8. Expression of GFP also was observed in vegetative hyphae in axenic culture (Figure 8F). Expression analysis by reverse transcription–mediated polymerase chain reaction confirmed the expression of *PDE1* during appressorium formation and was indicative of a higher level of *PDE1* expression compared with mycelium (data not shown). Sequence analysis of the *PDE1* promoter revealed the presence of a number of putative regulatory motifs consistent with expression of the gene during spore development. Two consensus stuA binding sites were present at positions −179 and −512, and two near-consensus binding sites for abaA were present at positions −390 and −746. *Stunted* (*stuA*) and *Abacus* (*abaA*) both encode transcriptional regulators involved in the spatial control of conidiation in the filamentous ascomycete fungus *Aspergillus nidulans* (Adams et al., 1998). We conclude that low-level *PDE1* expression occurs during vegetative growth and also throughout conidial germination and appressorium formation by Magnaporthe. The presence of a number of putative regulatory motifs is consistent with the expression of *PDE1* during spore development.

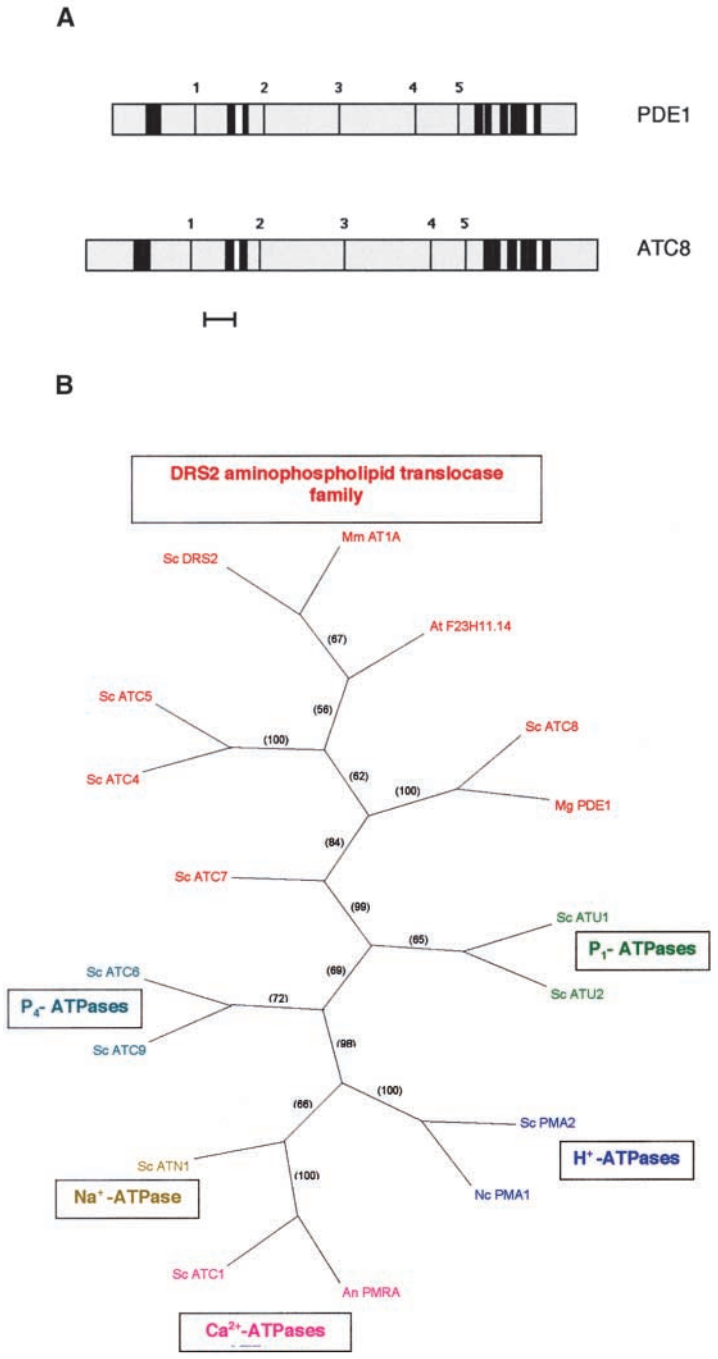

Figure 5. Predicted Topology of the Magnaporthe *PDE1* and *S. cerevisiae ATC8* Gene Products and Phylogenetic Tree of P-Type ATPases.

(A) The PredictProtein program (Rost et al., 1995) was used to make predictions of the transmembrane helices and topology of the putative PDE1 and ATC8 gene products. Transmembrane spans are indicated by thick black lines. Putative cytoplasmic domains are shown in gray, and extracytoplasmic regions are shown in white. The P-type consensus motifs are indicated by thin black lines: 1, LTGET motif; 2, DKTGTLT phosphorylation site; 3, KGA nucleotide binding site; 4, mLTGD ATP binding motif; 5, GDGXND hinge motif (Catty et al., 1997). Bar = 100 amino acids.
(B) Strict consensus phylogram of the most parsimonious tree showing relationships between P-type ATPases based on amino acid sequence. Relationships were determined by maximum parsimony using the heuristic search program with branch swapping and total branch recombination in PAUP version 4.0 (Swofford, 2000). Branch strengths were tested by 100 repetitions of the bootstrap algorithm with branch swapping. Numbers in parentheses are percentage bootstrap values. DRS2 aminophospholipid translocase family ATPases are shown in red: Mm AT1A,

DISCUSSION

The process of appressorium development by Magnaporthe has received considerable attention, and a rudimentary outline of the signaling apparatus necessary for appressorium elaboration and turgor generation is beginning to emerge. Appressoria form in response to physical and chemical cues from the plant surface that are detected by membrane components, including the product of the *PTH11* gene (DeZwaan et al., 1999). Strong attachment of the germ tube to the leaf surface and alterations in cell wall conformation, mediated in part by the MPG1 hydrophobin, contribute to surface perception (Hamer et al., 1988; Talbot et al., 1996), and the outcome is rapid activation of a G-protein-adenylate cyclase-cAMP–dependent signaling pathway. This, in turn, triggers multiple mitogen-activated protein kinase cascades, resulting in differentiation of the appressorium, transport of lipid and carbohydrate reserves to the infection cell, and generation of appressorial turgor (Mitchell and Dean, 1995; Xu and Hamer, 1996; Choi and Dean, 1997; Liu and Dean, 1997; Xu et al., 1997, 1998; Adachi and Hamer, 1998; Dixon et al., 1999; Thines et al., 2000). How appressorium development culminates in plant infection, however, is less clear because the genetic components required for penetration peg formation have not yet been identified.

Our aim in this study was to identify and characterize the *PDE1* gene, which had been defined previously by identification of an insertional mutant impaired in plant infection (Balhadère et al., 1999). When we analyzed the plant infection process in *pde1* mutants at the ultrastructural level, we found that cuticle penetration was reduced dramatically, and the only penetration structures observed were nonpolarized hyphae that were limited to the initial epidermal cell. The mutant phenotype, therefore, indicates that *PDE1* encodes a protein involved in the elaboration of penetration hyphae from the base of the appressorium during plant infection.

The original *pde1* mutation was caused by insertion of a plasmid into the promoter of the *PDE1* gene. Therefore, we could not be confident that the mutation had completely eliminated the biological activity of the *PDE1* gene product. A putative loss-of-function allele of *PDE1* was created by gene disruption, inserting a 1.4-kb selectable marker gene cassette into the first *PDE1* exon. Targeted disruption of *PDE1* in Magnaporthe strain Guy11 confirmed that the gene encodes a virulence factor for rice blast disease. The only disease symptoms observed after inoculation of rice with *pde1*::*Hph* mutants were small necrotic flecks similar to those found in a resistance response (Valent et al., 1991). There were, however, important differences in the characteristics of the original *pde1* mutant 2029 formed in a 35-R-24 genetic background and the *pde1*::*Hph* mutants made in Guy11. Strain 35-R-24 is a barley pathogenic form of Magnaporthe generated by selection and genetic backcrossing for increased symptom development on barley; it is not pathogenic on rice (Lau and Hamer, 1996). In contrast, Guy11 is a wild-type isolate of the fungus that is pathogenic on both rice and barley (Leung et al., 1988). Guy11 *pde1*::*Hph* mutants were reduced in their virulence toward rice but not toward barley.

In view of the difference in behavior of the two *pde1* mutants, we sequenced *PDE1* alleles from both Guy11 and 35-R-24 to determine whether the *PDE1* gene product might be distinct in each strain. Sequence analysis, however, showed a relatively high level of sequence conservation, including the maintenance of all of the P-type ATPase consensus sequences in each allele. This suggests that both *PDE1* alleles are functionally conserved. Consistent with this, the *pde1* mutant 2029 could be complemented by expression of a Guy11 *PDE1* allele. However, we cannot preclude the possibility that one of the five mutations in the *PDE1* coding sequence affects the specificity of its action in each Magnaporthe strain. Reciprocal complementation experiments are under way to address this possibility.

Another explanation for the *pde1* mutant phenotype differences, however, might be that a promoter insertion in *PDE1* is more deleterious to its role in barley infection than a loss-of-function mutation. We do not know the effect of the promoter insertion in mutant 2029 on *PDE1* expression

Figure 5. (continued).

Mus musculus chromaffin granule ATPase II AT1A (SWISS-PROT accession number P70704); At F23H11.14, *Arabidopsis thaliana* putative ATPase F23H11.14 (GenBank accession number AC007258); Sc ATC8, *Saccharomyces cerevisiae* ATC8 (SWISS-PROT accession number Q12674); Mg PDE1, *Magnaporthe grisea* PDE1 (this study); Sc DRS2, *S. cerevisiae* DRS2 (SWISS-PROT accession number P39524); Sc ATC4, *S. cerevisiae* ATC4 (SWISS-PROT accession number Q12675); Sc ATC5, *S. cerevisiae* ATC5 (SWISS-PROT accession number P32660); Sc ATC7, *S. cerevisiae* ATC7 (SWISS-PROT accession number P40527). P_1-ATPases are shown in green: Sc ATU1, *S. cerevisiae* copper-transporting ATPase ATU1 (SWISS-PROT accession number P38360); Sc ATU2, *S. cerevisiae* copper-transporting ATPase ATU2 (SWISS-PROT accession number P38995). H^+-ATPases are shown in blue: Sc PMA2, *S. cerevisiae* plasma membrane proton ATPase PMA2 (SWISS-PROT accession number P19657); Nc PMA1, *Neurospora crassa* plasma membrane proton ATPase PMA1 (SWISS-PROT accession number P07038). Ca^{2+}-ATPases are shown in pink: An PMRA, *Aspergillus niger* secretory pathway calcium ATPase PMRA (GenBank accession number AF232827); Sc ATC1, *S. cerevisiae* calcium-transporting ATPase ATC1 (SWISS-PROT accession number P13586). Na^+-ATPases are shown in dark yellow: Sc ATN1, *S. cerevisiae* sodium-transporting ATPase ATN1 (SWISS-PROT accession number P13587). P_4-ATPases are shown in turquoise: Sc ATC 6, *S. cerevisiae* cation-transporting ATPase ATC6 (SWISS-PROT accession number P39986); Sc ATC9, *S. cerevisiae* cation-transporting ATPase ATC9 (SWISS-PROT accession number Q12697).

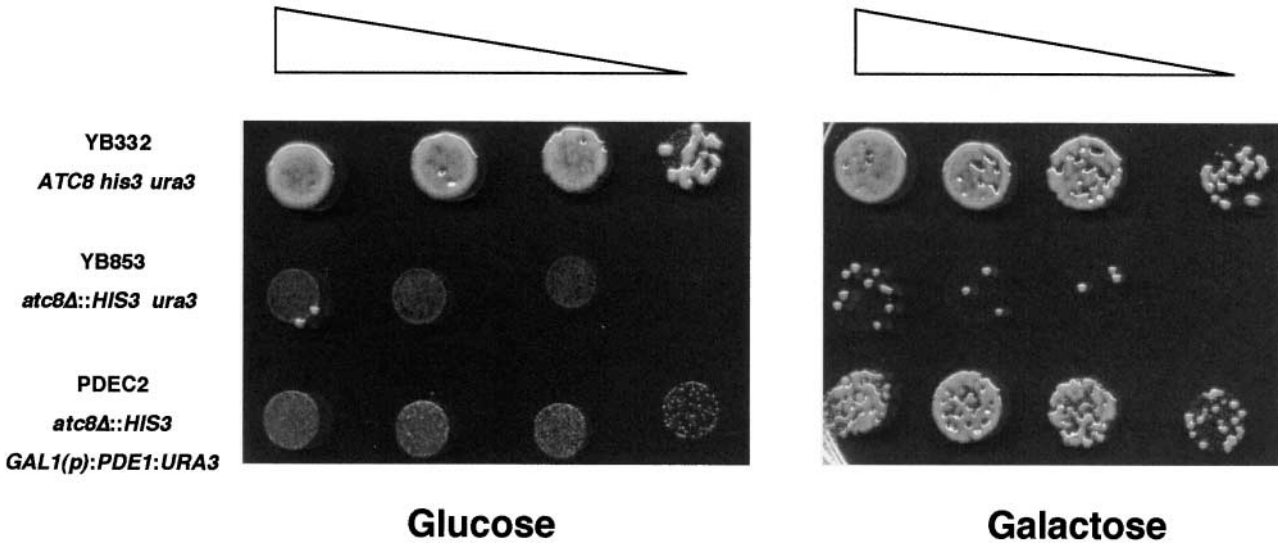

Figure 6. The Magnaporthe *PDE1* Gene Is a Functional Homolog of the *S. cerevisiae* P-Type ATPase Gene *ATC8*.

Growth of *S. cerevisiae* on glucose- or galactose-amended growth medium plates. Plate cultures were inoculated with 10-μL droplets containing 2×10^4, 10^4, 5×10^3, and 10^3 cells and were left to grow for 17 hr before examination. Triangles show the decreasing concentration of inoculum. Strain YB322 is a wild-type *S. cerevisiae* strain. YB853 is an *atc8Δ* P-type ATPase mutant. Strain PDEC2 is a transformant of YB853 expressing Magnaporthe *PDE1* under the control of the *S. cerevisiae* galactose-inducible *GAL1* promoter.

because the gene is not expressed sufficiently for the transcript to be detectable by RNA gel blot analysis. Mistimed gene expression or lack of induction, however, is a possible consequence of such a promoter insertion (Urban et al., 1999) and might be the cause of distinct mutant phenotypes. Targeted disruption of *PDE1* in 35-R-24 and introgression of the REMI allele from 2029 into a Guy11 background by genetic crosses are under way (M.J. Gilbert and N.J. Talbot, unpublished data) to determine the cause of plasticity in *PDE1* gene function.

There is a precedent in Magnaporthe for targeted gene mutations behaving distinctly in different strain backgrounds. The *PTH11* gene from Magnaporthe (DeZwaan et al., 1999) is involved in the regulation of appressorium formation on hydrophobic surfaces, but it appears to have a positive effect on appressorium morphogenesis in one Magnaporthe strain and to repress morphogenesis under different environmental conditions in another strain background (DeZwaan et al., 1999). Cellular signaling events for the expression of genes involved in plant infection, such as *PTH11* and *PDE1*, might be regulated distinctly in different host-limited forms of Magnaporthe.

PDE1 Encodes a Putative Aminophospholipid Translocase

Both sequence analysis and the complementation of a *atc8Δ* mutant indicate that *PDE1* encodes a P-type ATPase belonging to the DRS2 family of aminophospholipid translocases. P-type ATPases are so named because of the phosphoenzyme intermediate formed during their activation and have been implicated in a number of transport and signaling processes. The best-known members of the group are H^+-ATPases and heavy metal transporters (for reviews, see Catty et al., 1997; Bevers et al., 1999; Nelson and Harvey, 1999). All P-type ATPases share a core structure, including the presence of a phosphorylation site, an ATP binding domain, and three other consensus sequences (Figure 5). The DRS2 class of P-type ATPases, including PDE1, share all of these consensus sequences, but they also possess several domains that show that they are structurally distinct (Catty et al., 1997). Transmembrane domains 4 and 6 of the DRS2 class of P-type ATPases contain hydrophobic or aromatic amino acids in intrabilayer positions, in contrast to the charged and polar amino acids found in cation-transporting P-type ATPases (Lutsenko and Kaplan, 1995; Daleke and Lyles, 2000). Based on these differences, the *DRS2* class has been proposed to represent a separate subfamily of P-type ATPases that transport lipids rather than cations (Tang et al., 1996). Consistent with this, phylogenetic analysis performed in this study (Figure 5B) and by others (Catty et al., 1997) indicates that the DRS2 family of P-type ATPases diverged from a primordial P-type ATPase to perform a distinct function (Daleke and Lyles, 2000). Biochemical studies, meanwhile, have now revealed that aminophospholipid translocases, purified from erythrocytes and chromaffin granules in mammals, are phosphatidylserine-inducible,

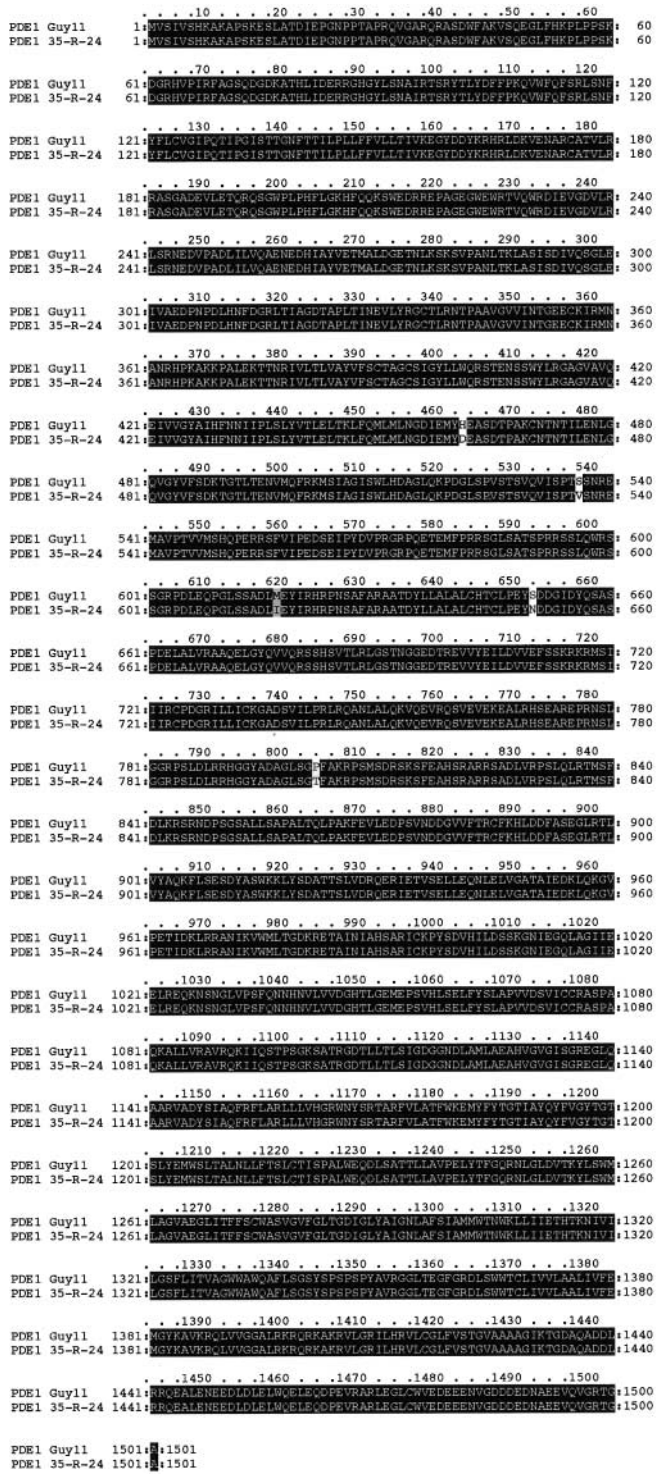

Figure 7. Alignment of the Predicted Amino Acid Sequence of *PDE1* Alleles from Magnaporthe Strains Guy11 and 35-R-24.

Sequences were aligned with the ClustalW program (Thompson et al., 1994). Identical amino acids are shown on a black background, and similar amino acids are shown on a light gray background. A high degree of amino acid conservation is present. In total, 45 nucleotide differences were observed between the alleles within the 4.6-kb region of the *PDE1* gene. This resulted in five nonsilent mutations, as indicated. All of the nonsilent mutations reside in the region corresponding to the large cytoplasmic loop between transmembrane domains 4 and 5. Each of the five conserved P-type ATPase consensus sequences is conserved in each allele. The 35-R-24 *PDE1* allele has GenBank accession number AF408935.

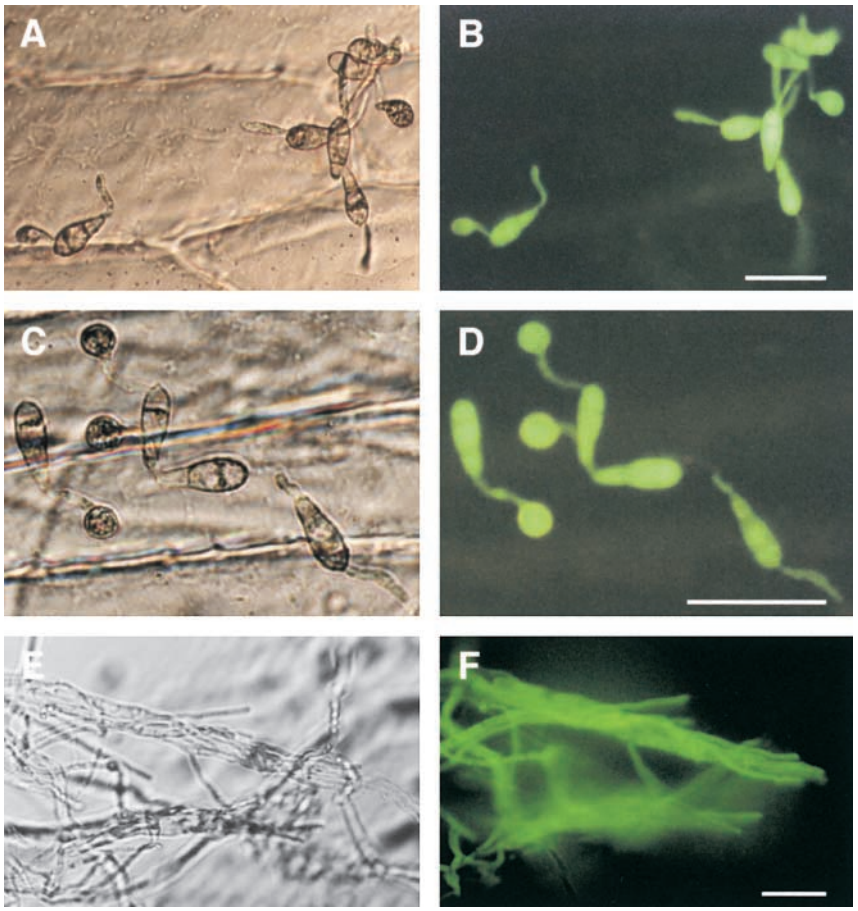

Figure 8. Spatial Regulation of *PDE1* Expression during Plant Infection and Vegetative Growth by Magnaporthe.

Conidia of a *PDE1(p)*::*sGFP*::*Hph* transformant PVG3 were incubated on sterile onion epidermis and allowed to form appressoria. Micrographs in **(A)**, **(C)**, and **(E)** at left are bright-field images viewed with Hoffman modulation optics (Nikon). GFP fluorescence is shown in **(B)**, **(D)**, and **(E)** at right.

(A) and **(B)** Germinated conidia with extended germ tubes 4 hr after inoculation.

(C) and **(D)** Conidia with fully formed appressoria 24 hr after inoculation.

(E) and **(F)** Hyphae grown in standard minimal medium for 48 hr.

Bars = 50 μm for all panels.

ATP-dependent, vanadate-sensitive Mg^{2+}-ATPase enzymes that correspond to products encoded by P-type ATPase genes clustering with the DRS2 family (Tang et al., 1996; Daleke and Lyles, 2000).

Aminophospholipid translocases are required to generate phospholipid asymmetry in membranes and therefore can act as key factors in determining membrane characteristics. A fundamental property of most biological membranes is the asymmetric distribution of lipids across the bilayer. Choline phospholipids (phosphatidylcholine and sphingomyelin) are localized predominantly in the outer monolayer of the plasma membrane (or the lumenal side of internal organellar membranes), whereas aminophospholipids (phosphatidylserine and phosphatidylethanolamine) are enriched on the inner (cytofacial) side of the plasma membrane. The asymmetric distribution of lipids provides both sides of a membrane with different characteristics, which are necessary for their different functions. The biological consequences of losing membrane asymmetry can be significant; apoptosis, for example, is accompanied by rapid loss of phospholipid asymmetry, which is required for recognition of apoptotic cells by macrophages (Bevers et al., 1999). The regulated disruption of phospholipid asymmetry consequently provides a pathway for cellular signaling in response to physiological conditions or environmental stresses.

Alternative Models for PDE1 Function during Appressorium-Mediated Plant Infection

The identification of *PDE1* indicates that maintenance of membrane asymmetry is important in penetration peg emergence. There are two plausible models that could account for the function of *PDE1* and the mutant phenotype encountered. During appressorium formation, the incipient appressorium demarcates the area of subsequent penetration peg emergence from the rest of the cell by its absence of a specialized cell wall (Bourett and Howard, 1990). This area, known as the appressorium pore, is a discrete, apparently wall-less zone at the base of the appressorium where the plasma membrane of the fungus appears to be in direct contact with the leaf surface. During penetration peg formation, the appressorium pore area is initially distended in a process that is accompanied by rapid cell wall biosynthesis at the apex of the penetration hypha (Bourett and Howard, 1990, 1992). The pore itself also becomes lined by a double layered cell wall at this time, known as the appressorium pore wall overlay. Based on this series of events and on the fact that penetration peg formation requires huge turgor pressure, it seems likely that the appressorium pore is subject to extreme membrane stress.

The maintenance of membrane asymmetry by a plasma membrane–localized *PDE1*-encoded ATPase might be required for the rapid alteration in membrane conformation that occurs during polarity establishment and formation of the penetration hypha. The appressorium pore membrane effectively changes from a flattened structure in contact with the leaf surface to a narrow cylindrical structure that undergoes rapid cell wall biosynthesis and polarized growth through the tough plant cuticle. If *PDE1* encodes a plasma membrane aminophospholipid translocase, it might be a critical requirement for this reorientation of hyphal growth. The slight delay in conidial germination observed in *pde1* mutants is consistent with this potential role, because the *PDE1* product may act in a similar manner during initial germ tube emergence, a parallel developmental process. The requirement for an aminophospholipid translocase in the context of hyphal emergence would be consistent with the biphasic model for membrane function formulated by Sheetz and Singer (1974). They reasoned that membrane asymmetry was likely to be fundamental to any alteration in membrane conformation during development. Computer predictions indicate that PDE1 is likely to be localized to the plasma membrane (60.9% probability based on PsortII analysis; Nakai and Kanehisa, 1992), so it is plausible that it fulfills this role.

At this stage, however, we cannot preclude the possibility that *PDE1* has a different function that is more closely related to that of *DRS2* in yeast (Chen et al., 1999). *DRS2* was originally thought to encode a plasma membrane ATPase (Tang et al., 1996), but it is now known to encode an organellar aminophospholipid translocase involved in late Golgi function (Chen et al., 1999; Marx et al., 1999). *drs2Δ* mutants are lethal when combined in yeast strains with clathrin heavy chain mutant alleles and exhibit defects in endosomal and Golgi function, suggesting a role in endocytosis, and more specifically, the movement of vesicles from endosomes to vacuoles (Chen et al., 1999). In filamentous fungi, the endocytotic pathway may be required for polarized growth because of the need for membrane recycling. This has been strongly implied from studies in *Ustilago maydis* (Wedlich-Söldner et al., 2000) and *Uromyces fabae* (Hoffmann and Mendgen, 1998).

Membrane recycling may be particularly important during the very rapid transition in growth that accompanies penetration peg formation and the release of appressorial turgor. If *PDE1* is required for the efficient movement and docking of endosomal vesicles, then this too might account for its requirement in penetration peg formation. To distinguish between these two models for *PDE1* function, we are currently raising antibodies to the protein to determine its cellular localization (M.J. Gilbert, P.V. Balhadère, and N.J. Talbot, unpublished data). The ambiguity of epitope-tagging strategies

Table 1. Characteristics of Magnaporthe Strains Used in This Study

Strains	Characteristics	Source
Wild-type strains		
Guy11	Field strain, *MAT1-2* rice pathogen	Leung et al. (1988)
35-R-24	Laboratory strain, *MAT1-2* barley pathogen	Lau and Hamer (1996)
35-R-56	Laboratory strain, *MAT1-1* barley pathogen	Lau and Hamer (1996)
Mutants/recombinant strains		
2029	*pde1* mutant of 35-R-24; *MAT1-2*, *Hph*[a]	Balhadère et al. (1999)
2029-R-32	*pde1* mutant (F1 progeny of cross between 2029 and 35-R-56); *MAT1-1*, *Hph*	Balhadère et al. (1999)
PVB6.1	Transformant of 2029 expressing 6.48-kb fragment of *PDE1* locus; wild-type phenotype; sulfonylurea-resistant; *Hph*	This study
PV1 to PV4	*pde1*::*Hph* gene disruption mutants of Guy11	This study
PVG1 to PVG4	*PDE1(p)*::*sGFP*::*Hph* transformants of Guy11	This study

[a] Hygromycin B–resistant transformant.

for localizing P-type ATPases (Siegmund et al., 1998; Chen et al., 1999) indicates that this may be the most accurate means of determining the location of PDE1. The functional relationship to the *S. cerevisiae DRS2* gene also is being examined by complementation analysis. Together, these experiments should enable us to determine the precise function of *PDE1* during plant infection.

In summary, the identification of *PDE1* implicates a completely new class of enzyme in the process of plant infection by phytopathogenic fungi, which also may constitute a novel target for disease intervention. The P-type ATPases are among the best-studied proteins in terms of their topological and drug interaction features (Moller et al., 1996), and *PDE1* may encode a valuable enzyme for disease control studies.

METHODS

Storage and Manipulation of Fungal and Bacterial Strains

Wild-type and mutant strains of *Magnaporthe grisea* are stored in the laboratory of N.J. Talbot at the University of Exeter. Details of the isolates used in this study are given in Table 1. Standard growth and storage procedures for Magnaporthe were performed as described previously (Crawford et al., 1986; Talbot et al., 1993). *Escherichia coli* strains XL1-Blue from Stratagene (Cambridge, UK) and KW251 from Promega (Southampton, UK) were used for standard cloning and phage propagation, respectively. The YB853 mutant strain of *Saccharomyces cerevisiae (MAT**a** ura3-52 his3Δ200 ade2-101 lys2-801 leu2-3, 112 atc8Δ::HIS3*) and the YB332 isogenic wild-type strain (*MAT**a** ura3-52 his3Δ200 ade2-101 lys2-801 leu2-3, 112*) were kindly donated by Dr. K. Ashrafi (Department of Molecular Biology and Pharmacology, Washington University School of Medicine, St. Louis, MO). Both strains were maintained and cultivated according to standard methods (Rose et al., 1990).

Rice and Barley Infections

Ten-day-old seedlings of the barley (*Hordeum vulgare*) cultivar Golden Promise were infected with suspensions of Magnaporthe conidia prepared in 0.2% gelatin at a concentration of 5×10^4 conidia·mL^{-1} or 10^5 conidia·mL^{-1} for isolates from the Guy11 or 35-R-24 genetic backgrounds, respectively. Magnaporthe Guy11 isolates also were used to infect the rice (*Oryza sativa*) cultivar CO-39 at a concentration of 2.5×10^4 conidia·mL^{-1}. Details of the methods for plant inoculation and the scoring of blast disease symptoms have been described previously (Balhadère et al., 1999). Lesion density values from 10 randomly chosen 5-cm-long leaf tips were routinely recorded, and the mean values were compared by analysis of variance after transformation into Logx.

Assays for Infection-Related Morphogenesis

Appressorium-mediated penetration of onion (*Allium cepa*) epidermal strips and of detached barley leaves was assayed as described previously (Balhadère et al., 1999). Conidia were allowed to germinate in water droplets on the surface of epidermal strips, and the frequency of cuticle penetration was recorded after 24, 31, and 48 hr for onion epidermis and barley leaves. The formation of a penetration peg from individual appressoria was determined by microscopy using an Optiphot-2 compound microscope (Nikon, Kingston, UK) under bright-field illumination or Hoffman modulation contrast. The frequencies with which mutant strains of Magnaporthe formed penetration pegs and ruptured cuticle layers were compared using a χ^2 test (Sokal and Rohlf, 1981).

Low-Temperature Scanning Electron Microscopy

Infection and colonization of barley leaf tissue were visualized using cryoscanning electron microscopy. Briefly, leaf tips from blast-inoculated seedlings were detached from plants 72 hr after initial inoculation. The leaf tips were plunge-frozen in nitrogen slush and mounted on a cryostage at −168°C. Transverse sections were made by fracturing leaves with a microtome knife, and the leaves were then incubated under vacuum on the scanning electron microscope stage at −80°C for 10 min to allow sublimation to occur before being returned to −168°C for sputter coating with gold. Samples were viewed at low temperature (−160°C) with a scanning electron microscope (model S100; Cambridge Instruments, Cambridge, UK) modified with a cryostage (model CT1500C; Oxford Instruments, Witney, Oxon, UK).

DNA Isolation and Analysis

Genomic DNA was extracted from fungal mycelium by using a hexadecyltrimethylammonium bromide procedure described by Talbot et al. (1993). Extraction of DNA from *S. cerevisiae* was performed according to a standard protocol (Rose et al., 1990). RNA was extracted from Magnaporthe according to the method of Timberlake (1980). Gel electrophoresis, restriction enzyme digestion, and DNA gel blot hybridization were all performed using standard procedures (Sambrook et al., 1989). DNA hybridization probes were labeled by the random primer method (Feinberg and Vogelstein, 1983) using the Stratagene Prime-It kit, and high-stringency washes were performed as described previously (Talbot et al., 1993). DNA sequencing was performed using a ABI 377 automated sequencer (Perkin-Elmer, Norwalk, CT) with ABI PRISM BigDye Terminator cycle sequencing (Applied Biosystems, Foster City, CA). DNA/protein sequence databases were searched using the BLAST algorithm (Altschul et al., 1990) at the National Center for Biotechnology Information (Bethesda, MD), which was accessed via the World Wide Web. Nucleic acid sequences also were analyzed for the presence of introns with SpliceView (Rogozin and Milanesi, 1997) for the prediction of TATA signals with the HCtata algorithm and for poly(A) signals with the HCpolya algorithm (Milanesi et al., 1996), all of which are available at the WebGene server of the Istituto Tecnologie Biomediche Avanzate (Segrate, Italy). The promoter sequence was dissected using the MatInspector algorithm (Quandt et al., 1995) accessed at the Forshungszentrum für Umwelt und Gesundheit (Neuherberg, Germany). The protein molecular weight was predicted with the Computepl/Mw program (Wilkins et al., 1998) available on the ExPASy proteomics server of the Schweizerisches Institut für Bioinformatik (Geneva, Switzerland). Amino acid alignments were produced using ClustalW (Thompson et al., 1994), available at the Network Protein Sequence @nalysis site in the Pôle Bioinformatique Lyonnais (Lyon, France). Phylogenetic analysis was performed by maximum parsimony using

the heuristic search program with branch swapping and total branch recombination in PAUP version 4.0 (Swofford, 2000). Branch strength was tested by 100 repetitions of the bootstrap algorithm with branch swapping. Secondary protein structure analysis was performed using the program PredictProtein (Rost et al., 1995) available at the EMBL server (Heidelberg, Germany). Protein subcellular localization was predicted using PsortII (Nakai and Kanehisa, 1992) at the Okasaki server (Japan).

Identification of the *PDE1* Gene

The candidate *PDE1* locus was recovered from the *pde1* mutant 2029 through a plasmid rescue strategy (Kuspa and Loomis, 1992). Mutant 2029 was generated in Magnaporthe strain 35-R-24 by transformation with pCB1003 (Carroll et al., 1994) in the presence of BamHI (Balhadère et al., 1999). Restriction mapping revealed the presence of a ClaI site that was absent in the vector; therefore, 2029 genomic DNA was digested with ClaI and religated using T4 DNA ligase (Promega) at 14°C. The ligated genomic DNA was used to transform *E. coli* XL1-Blue cells, and ampicillin-resistant transformants were selected that contained pCB1003 and a 550-bp region of Magnaporthe chromosomal DNA flanking the insertion site. This restriction fragment was radiolabeled and used to screen a Guy11 λ library (Talbot et al., 1993) to obtain a genomic clone. After restriction mapping of the candidate locus, several fragments (a 2.6-kb PstI, a 3.3-kb SalI, a 2.6-kb XhoI, and a 1.8-kb SalI fragment spanning a contiguous 6.94-kb region) were subcloned into pBluescript II SK− phagemid (Stratagene), generating plasmids pSKP1, pSKS1, pSKX1, and pSKS2. Each subcloned fragment was prepared for sequencing using the GPS-1 genome priming system (New England Biolabs, Hitchin, UK).

The *PDE1* gene was reintroduced into *pde1* mutant strains by using the following methods. A *PDE1* gene fragment containing 1.47 kb of promoter and 468 bp of terminator sequence was amplified from a Guy11 λ genomic clone using two EcoRI-linked primers, GF1 (5′-CGGAATTCGCCACGGCGGCCTACGAC-3′) and C3 (5′-GAATTC-CCTTCCCATCTTTGGTGTGC-3′). The polymerase chain reaction (PCR) was performed in a Perkin-Elmer GeneAmp PCR System 2400 cycler using a 25:1 (v:v) mixture of Taq:TurboPfu DNA polymerases (with 2.5 units of Taq per reaction and 0.1 unit of TurboPfu) by applying 25 amplification cycles, after a hot start of 3 min at 94°C in the absence of deoxynucleotide triphosphates, followed by a final 10-min extension at 72°C. Amplification conditions were as follows: 5 sec of denaturation at 95°C, 30 sec of annealing at 67°C, and 6 min of elongation at 68°C. The resulting 6.48-kb amplicon was cloned into pGEM-T (Promega).

The pPDE1 construct was linearized with NotI and used in cotransformation experiments with the plasmid pGEM-ILV1 (A.J. Foster, unpublished data), which contained a Magnaporthe *ILV1* allele conferring sulfonylurea resistance, amplified from plasmid pCB1254 (Sweigard et al., 1998). The latter plasmid was a generous gift from Dr. James A. Sweigard (Central Research and Development Department, DuPont, Wilmington, DE). Cotransformation experiments were performed using strain 2029-32 (a *pde1* progeny described by Balhadère et al., 1999). Protoplasts were plated on defined complex medium in the presence of chlorimuron ethyl at 100 $\mu g \cdot mL^{-1}$ as described by Sweigard et al. (1997). Sulfonylurea-resistant transformants were screened for the presence of pPDE1 by PCR amplification of genomic DNA templates with primers GF1 and GF2 (5′-CCCATGGTGCCGCTAGCTTTTGCAACG-3′). The latter primer anneals to the *PDE1* translation initiation codon sequence, and the primers should enable amplification of a 5.6-kb fragment from the *pde1* insertional mutant locus and a 1.5-kb fragment from the integrated plasmid. The introduction of pPDE1 was confirmed subsequently by DNA gel blot analysis (data not shown).

Targeted Gene Disruption of *PDE1*

Construction of the pPde1::Hph disruption vector was performed by first generating the pSKP2 plasmid by cloning the 2.6-kb PstI fragment from pSKP1 (containing 1.87 kb of promoter sequence and 0.73 kb of the *PDE1* protein-coding sequence) into an engineered pBluescript II SK− (lacking SmaI, BamHI, SpeI, or XbaI sites in the polylinker). The 1.4-kb hygromycin phosphotransferase gene cassette was amplified from pCB1003 by using primers hygafl1 (5′-CCA-GACATGTCACGACGTTGTAAAA-3′) and hygafl2 (5′-CCAGACATG-TGTCGACTCTAGAGG-3′). The amplification program consisted of 30 cycles (1 min of denaturation at 94°C, 1 min of annealing at 59°C, and a 1-min extension at 72°C) using 1.5 units of Pfu DNA polymerase (Promega) per reaction. The amplicon was directly blunt-end cloned into the unique SmaI site present in pSKP2 (69 bp downstream of the *PDE1* start codon), introducing a TAG stop codon 18 bp beyond the insertion site and creating pΔPDE1 (Figure 2). The recombinant plasmid pPde1::Hph was linearized with HindIII for subsequent use in fungal transformation. Fungal transformations were performed as described by Talbot et al. (1993) using hygromycin B (Calbiochem, Nottingham, UK) as a selective marker at a final concentration of 100 $\mu g \cdot mL^{-1}$. Transformants were selected 7 days later, and DNA gel blot analysis was performed to determine whether targeted disruption of *PDE1* had taken place. Sequence analysis was used to confirm creation of the insertion allele.

Complementation of the *S. cerevisiae atc8Δ* Mutation

To generate the pYESPDE1 complementation vector, a 4.6-kb DNA fragment spanning the entire *PDE1* protein-coding region was first amplified and cloned into pGEM-T. The amplicon was generated using genomic clone λPVB3 as a template and EcoRI-linked primers C1 (5′-GAATTCGGGCAGACGTTGCAAAAGC-3′) and C2 (5′-GAA-TTCTCAAGCCCCTGTTCGGCCG-3′). The amplicon contained the full *PDE1* open reading frame and a stretch of 27 bp in the 5′ untranslated region, which contained a Kozak translation initiation sequence. Amplification proceeded as described above, with annealing at 63.5°C and elongation for 5 min. The amplicon was cloned into the EcoRI site of the pYES2 expression vector (Invitrogen, Carlsbad, CA), downstream of the yeast *GAL1* promoter, to create pYESPDE1. The fidelity of the insertion was confirmed by DNA sequence analysis.

The pYESPDE1 vector was introduced into *S. cerevisiae* strain YB853 (*atc8Δ*) by using a small-scale yeast transformation protocol (Invitrogen) adapted from Rose et al. (1990). Uracil prototrophic yeast transformants were checked for the presence of pYESPDE1 by both PCR and DNA gel blot analysis (data not shown). No specific phenotype has been ascribed to the *atc8Δ* mutant YB853 (Ashrafi et al., 1998), but close inspection of its growth pattern compared with that of the isogenic wild-type strain YB332 revealed that YB853 showed a longer lag phase on both glucose- and galactose-supplemented yeast peptone dextrose (YPD) medium, corresponding to 2.5 to 3 hr. To check for complementation of this growth phenotype, the following experimental protocol was followed. Yeast cultures were prepared

overnight in liquid YPD in the presence of 2% glucose at 29°C with aeration at 150 rpm. The cells were then diluted to a final concentration of 4×10^5 cells·mL^{-1} in liquid YPD containing either 2% glucose or 2% galactose and grown with shaking for a period of 8 to 10 hr to enable galactose-induced expression of the *GAL1(p)*:*PDE1* allele. The cells were then serially diluted on glucose- or galactose-amended YPD plates (10-μL droplets containing 2×10^4, 10^4, 5×10^3, and 10^3 cells) and left to grow for 17 hr before examination.

PDE1 Expression Analysis

For construction of the pPDE1p-sGFP plasmid, a 1.47-kb promoter sequence from the 5′ end of *PDE1* was amplified from Guy11 genomic DNA and cloned into pGEM-T to create pPDE(p)-1. Conditions of amplification involved 1 min of annealing at 59°C and a 2-min extension at 72°C using 2.5 units of Taq DNA polymerase and the EcoRI-linked GF1 and NcoI-linked GF2 primers (as shown previously). The pPDE(p)-1 EcoRI-NcoI insert was cloned upstream of the *sGFP* gene–*TrpC* terminator cassette from plasmid pMJK-80 (Kershaw et al., 1998). The pPDE1p-sGFP plasmid was generated by releasing the gene fusion insert as a 2.8-kb EcoRI-KpnI fragment and cloning this into pCB1265, which carries the *bar* gene, which confers resistance to bialaphos (Sweigard et al., 1997). The pPDE1p-sGFP plasmid was introduced into Magnaporthe strain Guy11, and transformants were analyzed using DNA gel blots to ensure the integration of a single copy of the plasmid. Four independent transformants were examined by microscopy with similar results. Reverse transcription–mediated PCR was conducted on total RNA extracted from Magnaporthe mycelial cultures or appressoria using an Advantage RT-for-PCR kit (Clontech, Basingstoke, UK).

ACKNOWLEDGMENTS

We thank Richard Ward and Gavin E. Wakley for scanning electron microscopy, Dr. Fabian Seymour for phylogenetic analysis, and Dr. Andrew J. Foster and Nick Tongue for help with some of the cloning procedures. This work was supported by Grant 9/P14077 to N.J.T. from the Biotechnology and Biological Sciences Research Council. Work on rice blast in N.J.T's laboratory is authorized by the Plant Health Division of the Ministry of Agriculture, Fisheries, and Food (License PHF 4343A/3551-8/2000).

Received February 12, 2001; accepted June 13, 2001.

REFERENCES

Adachi, K., and Hamer, J.E. (1998). Divergent cAMP signaling pathways regulate growth and pathogenesis in the rice blast fungus *Magnaporthe grisea*. Plant Cell **10,** 1361–1373.

Adams, T.H., Wieser, J.K., and Yu, J.H. (1998). Asexual sporulation in *Aspergillus nidulans*. Microbiol. Mol. Biol. Rev. **62,** 35–54.

Altschul, S.F., Gish, W., Miller, W., Myers, C.W., and Lipman, D.L. (1990). Basic local alignment search tool. J. Mol. Biol. **215,** 403–410.

Ashrafi, K., Farazi, T.A., and Gordon, J.I. (1998). A role for *Saccharomyces cerevisiae* fatty acid activation protein 4 in regulating protein N-myristoylation during entry into stationary phase. J. Biol. Chem. **273,** 25864–25874.

Balhadère, P.V., Foster, A.J., and Talbot, N.J. (1999). Identification of pathogenicity mutants of the rice blast fungus *Magnaporthe grisea* by insertional mutagenesis. Mol. Plant-Microbe Interact. **12,** 129–142.

Bechinger, C., Giebel, K.-F., Schnell, M., Leiderer, P., Deising, H.B., and Bastmeyer, M. (1999). Optical measurements of invasive forces exerted by appressoria of a plant pathogenic fungus. Science **285,** 1896–1899.

Bevers, E.M., Comfurius, P., Dekkers, D.W.C., and Zwaal, R.F.A. (1999). Lipid translocation across the plasma membrane of mammalian cells. Biochim. Biophys. Acta **1439,** 317–330.

Bourett, T.M., and Howard, R.J. (1990). *In vitro* development of penetration structures in the rice blast fungus *Magnaporthe grisea*. Can. J. Bot. **68,** 329–342.

Bourett, T.M., and Howard, R.J. (1992). Actin in penetration pegs of the fungal rice blast pathogen, *Magnaporthe grisea*. Protoplasma **168,** 20–26.

Carroll, A.M., Sweigard, J.A., and Valent, B. (1994). Improved vectors for selecting resistance to hygromycin. Fungal Genet. Newsl. **41,** 22.

Catty, P., de Kerchove d'Exaerde, A., and Goffeau, A. (1997). The complete inventory of the yeast *Saccharomyces cerevisiae* P-type transport ATPases. FEBS Lett. **409,** 325–332.

Chen, C.Y., Ingram, M.F., Rosal, P.H., and Graham, T.R. (1999). Role for Drs2p, a P-type ATPase and potential aminophospholipidtranslocase, in yeast late Golgi function. J. Cell Biol. **147,** 1223–1236.

Chida, T., and Sisler, H.D. (1987). Restoration of appressorial penetration ability by melanin precursors in *Pyricularia oryzae* treated with antipenetrants and in melanin-deficient mutants. J. Pestic. Sci. **12,** 49–55.

Chiu, W.L., Niwa, Y., Zeng, W., Hirano, T., Kobayashi, H., and Sheen, J. (1996). Engineered GFP as a vital reporter in plants. Curr. Biol. **6,** 325–330.

Choi, W., and Dean, R.A. (1997). The adenylate cyclase gene *MAC1* of *Magnaporthe grisea* controls appressorium formation and other aspects of growth and development. Plant Cell **9,** 1973–1983.

Chumley, F.G., and Valent, B. (1990). Genetic analysis of melanin deficient, nonpathogenic mutants of *Magnaporthe grisea*. Mol. Plant-Microbe Interact. **3,** 135–143.

Crawford, M.S., Chumley, F.G., Weaver, C.G., and Valent, B. (1986). Characterization of the heterokaryotic and vegetative diploid phases of *Magnaporthe grisea*. Genetics **114,** 1111–1129.

Daleke, D.L., and Lyles, J.V. (2000). Identification and purification of aminophospholipid flippases. Biochim. Biophys. Acta **1486,** 108–127.

Davenport, K.R., Sohaskey, M., Kamada, Y., Levin, D.E., and Gustin, M.C. (1995). A second osmosensing signal transduction pathway in yeast: Hypotonic shock activates the PKC1 protein kinase-regulated cell integrity pathway. J. Biol. Chem. **270,** 30157–30161.

Dean, R.A. (1997). Signal pathways and appressorium morphogenesis. Annu. Rev. Phytopathol. **35,** 211–234.

de Jong, J.C., McCormack, B.J., Smirnoff, N., and Talbot, N.J. (1997). Glycerol generates turgor in rice blast. Nature **389,** 244–245.

DeZwaan, T.M., Carroll, A.M., Valent, B., and Sweigard, J.A. (1999). *Magnaporthe grisea* Pth11p is a novel plasma membrane protein that mediates appressorium differentiation in response to inductive surface cues. Plant Cell **11,** 2013–2030.

Dixon, K.P., Xu, J.-R., Smirnoff, N., and Talbot, N.J. (1999). Independent signaling pathways regulate cellular turgor during hyperosmotic stress and appressorium-mediated plant infection by the rice blast fungus *Magnaporthe grisea*. Plant Cell **11,** 2045–2058.

Feinberg, A.P., and Vogelstein, B. (1983). A technique for radiolabeling DNA restriction endonuclease fragments to high specific activity. Anal. Biochem. **132,** 6–13.

Hamer, J.E., and Talbot, N.J. (1998). Infection-related development in the rice blast fungus *Magnaporthe grisea*. Curr. Opin. Microbiol. **1,** 693–697.

Hamer, J.E., Howard, R.J., Chumley, F.G., and Valent, B. (1988). A mechanism for surface attachment of spores of a plant pathogenic fungus. Science **239,** 288–290.

Heath, M.C., Valent, B., Howard, R.J., and Chumley, F.G. (1990). Interactions of two strains of *Magnaporthe grisea* with rice, goosegrass and weeping lovegrass. Can. J. Bot. **68,** 1627–1637.

Hoffmann, J., and Mendgen, K. (1998). Endocytosis and membrane turnover in the germ tube of *Uromyces fabae*. Fungal Genet. Biol. **24,** 77–85.

Howard, R.J., and Ferrari, M.A. (1989). Role of melanin in appressorium formation. Exp. Mycol. **13,** 403–418.

Howard, R.J., and Valent, B. (1996). Breaking and entering: Host penetration by the fungal rice blast pathogen *Magnaporthe grisea*. Annu. Rev. Microbiol. **50,** 491–512.

Howard, R.J., Ferrari, M.A., Roach, D.H., and Money, N.P. (1991). Penetration of hard substrates by a fungus employing enormous turgor pressures. Proc. Natl. Acad. Sci. USA **88,** 11281–11284.

Kershaw, M.J., Wakley, G.E, and Talbot, N.J. (1998). Complementation of the *Mpg1* mutant phenotype *in Magnaporthe grisea* reveals functional relationships between fungal hydrophobins. EMBO J. **17,** 3838–3849.

Kuspa, A., and Loomis, W.F. (1992). Tagging developmental genes in *Dictyostelium* by restriction enzyme-mediated integration of plasmid DNA. Proc. Natl. Acad. Sci. USA **89,** 8803–8807.

Lau, G.W., and Hamer, J.E. (1996). Regulatory genes controlling *MPG1* expression and pathogenicity in the rice blast fungus *Magnaporthe grisea*. Plant Cell **8,** 771–781.

Leung, H., Borromeo, E.S., Bernardo, M.A., and Notteghem, J.-L. (1988). Genetic analysis of virulence in the rice blast fungus *Magnaporthe grisea*. Phytopathology **78,** 1227–1233.

Liu, S., and Dean, R.A. (1997). G protein α-subunit genes control growth, development and pathogenicity of *Magnaporthe grisea*. Mol. Plant-Microbe Interact. **10,** 1075–1086.

Lutsenko, S., and Kaplan, J.H. (1995). Organization of P-type ATPases: Significance of structural diversity. Biochemistry **34,** 15607–15613.

Marx, U., Polakowski, T., Pomorski, T., Lang, C., Nelson, H., Nelson, N., and Herrmann, A. (1999). Rapid transbilayer movement of fluorescent phospholipid analogues in the plasma membrane of endocytosis-deficient yeast cells does not require the Drs2 protein. Eur. J. Biochem. **263,** 254–263.

Mendgen, K., Hahn, M., and Deising, H. (1996). Morphogenesis and mechanisms of penetration by plant pathogenic fungi. Annu. Rev. Phytopathol. **34,** 367–386.

Milanesi, L., Muselli, M., and Arrigo, P. (1996). Hamming clustering method for signals prediction in 5′ and 3′ regions of eukaryotic genes. Comput. Appl. Biosci. **12,** 399–404.

Mitchell, T.K., and Dean, R.A. (1995). The cAMP-dependent protein kinase catalytic subunit is required for appressorium formation and pathogenesis by the rice blast fungus *Magnaporthe grisea*. Plant Cell **7,** 1869–1878.

Moller, J.V., Juul, B., and le Maire, M. (1996). Structural organization, ion transport, and energy transduction of P-type ATPases. Biochim. Biophys. Acta **1286,** 1–51.

Nakai, K., and Kanehisa, M. (1992). A knowledge base for predicting protein localisation sites in eukaryotic cells. Genomics **14,** 897–911.

Nelson, N., and Harvey, W.R. (1999). Vacuolar and plasma membrane proton-adenosinetriphosphatases. Physiol. Rev. **79,** 361–385.

Paulsen, I.T., Sliwinski, M.K., Nelissen, B., Goffeau, A., and Saier, M.H. (1998). Unified inventory of established and putative transporters encoded within the complete genome of *Saccharomyces cerevisiae*. FEBS Lett. **430,** 116–125.

Quandt, K., Frech, K., Karas, H., Wingender, E., and Werner, T. (1995). MatInd and MatInspector: New fast and versatile tools for detection of consensus matches in nucleotide sequence data. Nucleic Acids Res. **23,** 4878–4884.

Rogozin, I.B., and Milanesi, L. (1997). Analysis of donor splice signals in different organisms. J. Mol. Evol. **45,** 50–59.

Rose, M.D., Winston, F., and Hieter, P. (1990). Methods in Yeast Genetics: A Laboratory Course Manual. (Cold Spring Harbor, NY: Cold Spring Harbor Laboratory Press).

Rost, B., Casadio, R., Fariselli, P., and Sander, C. (1995). Transmembrane helices predicted at 95-percent accuracy. Protein Sci. **4,** 521–533.

Sambrook, J., Fritsch, E.F., and Maniatis, T. (1989). Molecular Cloning: A Laboratory Manual. (Cold Spring Harbor, NY: Cold Spring Harbor Laboratory Press).

Sheetz, M.P., and Singer, S.J. (1974). Biological membranes as bilayer couples: A molecular mechanism of drug-erythrocyte interactions. Proc. Natl. Acad. Sci. USA **71,** 4457–4461.

Siegmund, A., Grant, A., Angeletti, C., Malone, L., Nichols, J.W., and Rudolph, H.K. (1998). Loss of Drs2p does not abolish transfer of fluorescence-labeled phospholipids across the plasma membrane of *Saccharomyces cerevisiae*. J. Biol. Chem. **273,** 34399–34405.

Sokal, R.R., and Rohlf, F.J. (1981). Biometry. (San Francisco, CA: W.H. Freeman and Company).

Sweigard, J., Chumley, F., Carroll, A., Farrall, L., and Valent, B. (1997). A series of vectors for fungal transformation. Fungal Genet. Newsl. **44,** 52–53.

Sweigard, J.A., Carroll, A.M., Farrall, L., Chumley, F.G., and Valent, B. (1998). *Magnaporthe grisea* pathogenicity genes obtained through insertional mutagenesis. Mol. Plant-Microbe Interact. **11,** 404–412.

Swofford, D.L. (2000). PAUP*: Phylogenetic Analysis Using Parsimony (* and Other Methods), Version 4. (Sunderland, MA: Sinauer Associates).

Talbot, N.J. (1995). Having a blast: Exploring the pathogenicity of *Magnaporthe grisea*. Trends Microbiol **3,** 9–16.

Talbot, N.J., Ebbole, D.J., and Hamer, J.E. (1993). Identification and characterization of *MPG1*, a gene involved in pathogenicity from the rice blast fungus *Magnaporthe grisea*. Plant Cell **5,** 1575–1590.

Talbot, N.J., Kershaw, M.J., Wakley, G.E., de Vries, O.M.H., Wessels, J.G.H., and Hamer, J.E. (1996). *MPG1* encodes a fungal hydrophobin involved in surface interactions during infection-related development of *Magnaporthe grisea*. Plant Cell **8,** 985–999.

Tang, X., Halleck, M.S., Schlegel, R.A., and Williamson, P.A. (1996). Subfamily of P-type ATPases with aminophospholipid transporting activity. Science **272,** 1495–1497.

Thines, E., Weber, R.W.S., and Talbot, N.J. (2000). MAP kinase and protein kinase A–dependent mobilization of triacylglycerol and glycogen during appressorium turgor generation by *Magnaporthe grisea*. Plant Cell **12,** 1703–1718.

Thompson, J.D., Higgins, D.G., and Gibson, T.J. (1994). ClustalW: Improving the sensitivity of progressive multiple sequence alignment through sequence weighting, position-specific gap penalties and weight matrix choice. Nucleic Acids Res. **22,** 4673–4680.

Timberlake, W.E. (1980). Developmental gene regulation in *Aspergillus nidulans*. Dev. Biol. **78,** 497–510.

Urban, M., Bhargava, T., and Hamer, J.E. (1999). An ATP-driven efflux pump is a novel pathogenicity factor in rice blast disease. EMBO J. **18,** 512–521.

Valent, B., Farrall, L., and Chumley, F.G. (1991). *Magnaporthe grisea* genes for pathogenicity and virulence identified through a series of backcrosses. Genetics **127,** 87–101.

Wedlich-Söldner, R., Bölker, M., Kahman, R., and Steinberg, G. (2000). A putative endosomal t-SNARE links ex- and endocytosis in the phytopathogenic fungus *Ustilago maydis*. EMBO J. **19,** 1974–1986.

Wilkins, M.R., Gasteiger, E., Bairoch, A., Sanchez, J.C., Williams, K.L., Appel, R.D., and Hochstrasser, D.F. (1998). Protein identification and analysis tools in the ExPASy server. In 2-D Proteome Analysis Protocol, A.J. Link, ed (Totawa, NJ: Humana Press).

Xu, J.-R., and Hamer, J.E. (1996). MAP kinase and cAMP signaling regulate infection structure formation and pathogenic growth in the rice blast fungus *Magnaporthe grisea*. Genes Dev. **10,** 2696–2706.

Xu, J.-R., Urban, M., Sweigard, J.A., and Hamer, J.E. (1997). The *CPKA* gene of *Magnaporthe grisea* is essential for appressorial penetration. Mol. Plant-Microbe Interact. **10,** 187–194.

Xu, J.-R., Staiger, C.J., and Hamer, J.E. (1998). Inactivation of the mitogen-activated protein kinase Mps1 from the rice blast fungus prevents penetration of host cells but allows activation of plant defense responses. Proc. Natl. Acad. Sci. USA **95,** 12713–12718.